



COBEM
2021 Florianópolis - Brasil



26th ABCM International Congress of Mechanical Engineering
November 22-26, 2021. Florianópolis, SC, Brazil

COB-2021-0200

Active Control of Oscillations in a Beam using Actuation by Macro Fiber Composites and Optimal Control

Lucas Zanovello Tahara
Arthur Silva Barbosa
Maíra Martins da Silva

School of Engineering of São Carlos, University of São Paulo, São Carlos
mairams@sc.usp.br

Abstract. *This paper aims to develop a model in the state-space of a flexible beam under piezoelectric actuation, which can be actively controlled using an optimal control strategy. Robotics has been growing at an accelerated rate in recent years, especially in robotics that aims at the interaction between humans and robots more safely. Under this context, soft robotics emerged to propose robots that need unstructured environments, which goes against traditional robotics. Therefore, this work presents a mathematical model of a beam with actuators that follow soft robotics' premises: high deformation capacity and low rigidity. The obtained simulations showed that, at the price of the increase in computational cost, the output reaches the desired references, which opens possibilities for using this type of system in robots that require high deformations. The use of MFCs proved to be efficient for the performance of soft systems, and the control strategy adopted allowed the optimization of inputs according to the desired outputs. The simulation algorithm's construction was done using the Python programming language, which allowed the algorithm's generalization for future work involving systems control under state-space formulation.*

Keywords: *Optimal Control, Macro Fiber Composites, Euler Bernoulli Beam, Active Control, Oscillation Control*

1. INTRODUCTION

The purpose of this work is to present an active control method on beams using piezoelectric actuators. The chosen actuators (Macro Fiber Composite, MFC) were developed at the NASA Research Center (NASA Langley Research Center, Wilkie *et al.* (2000)) in order to be structured with piezoelectric properties and, in parallel, have high flexibility (unlike conventional piezoelectric materials, such as ceramics, which have high values of modulus of elasticity).

As it is an active process, the control project aimed to reproduce the movement's reference of interest in the system. For this, an optimal control strategy was applied: Model Predictive Control (MPC). This control strategy minimizes a cost function responsible for calculating the performance required by the system. In the present study, the reference that the control must follow changes at each instant of a predetermined time, thus imitating the desired behavior.

The model considered for the study was that of a beam under the Euler-Bernoulli hypothesis with boundary conditions embed at one end and free at the other. The solution to this problem will be given through the variable separation method. This proposed solution is widely reported in the literature, as can be found in the authors' book Balachandran and Magrab (2018).

The differential of this work is a new proposal for the formulation of the system in state-space. Model-based control strategies can be explored using this formulation. This is the case of optimal control, where the designer can choose a cost function to minimize or maximize some property of interest (amplitude of vibration, energy used in control, rate of change of actuation).

The simulations showed that the adopted approach was efficient in controlling the movement of the system. The developed methodology can be applied to control vibrations or in areas that work with flexible systems, such as soft robotics, as shown in Gillespie *et al.* (2016), where a soft robot had its trajectory projected by the control strategy used in this work (MPC).

This work is divided into four sections: Section 2 presents the modeling of the system, and Section 3 the control strategy. Results are presented in Section 4, while conclusions are drawn in Section 5.

2. SYSTEM PROPOSAL AND MODELING

The term "intelligent" is linked to unusual properties of materials, the definition presented in Leo (2007) brings the following classification: a type of material will be classified as intelligent if it exhibits multiphysical coupling. In other

words, it can convert energy between multiple physical domains. The property of interest for the actuation of systems that connect the mechanical domain to the electrical domain is piezoelectricity.

Piezoelectricity is a property that can be used in a variety of applications, for example: harvesting (Erturk and Inman, 2011), actuation (Shahab and Erturk, 2016), (Shahab, 2015; Bent, 1997) and vibration control (Rimašauskienė *et al.*, 2019). The mathematical approach for the different applications is similar since the relationship between the physical domains (mechanical and electrical) is the same regardless of their use.

The use of ceramic actuators and sensors with piezoelectric properties has a limitation that restricts its applicability: low deformation. The density values for piezo ceramic materials have the same order of magnitude as metals such as aluminum or steel. Combined with low deformation, the low force imposition capacity also restricts the use of ceramic actuators in high deformation systems. To solve the problems involving the use of ceramic actuators, macro-fiber composites with piezoelectric characteristics (MFC) were created.

The piezoelectricity constitutive equation in ceramics foresee linear relationships between the inputs and outputs of the physical domains; however, this characteristic is untrue for the electric field between the piezoelectric fibers of the MFC. To get around this problem, some modeling proposals have been reported, such as in Bilgen *et al.* (2010), Bilgen *et al.* (2008) and Huang (2017). In general, the modeling revolves around defining a fraction of volume to study the properties and subsequent generalization for the entire body.

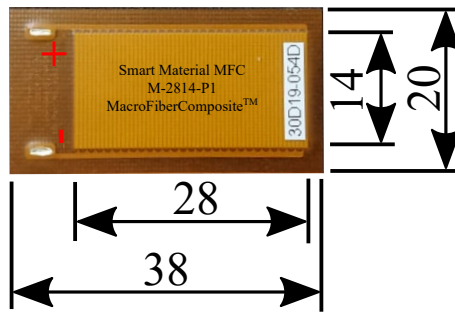


Figure 1. Macro Fiber Composite from Smart Material (2003 -2021) with dimensions in millimeters.

In this paper, the approach proposed by Deraemaeker *et al.* (2009) is adopted for the modeling of MFCs. Their proposal is to use equivalent properties for representative units of volume and the combination of their effects on the final behavior of the MFC. This approach was validated experimentally by Shahab (2015), where the electromechanical couplings estimated were analyzed in the laboratory.

2.1 PROTOTYPE AND HYPOTHESES ADOPTED

The proposed system is modeled using an Euler-Bernoulli beam (Fig. 2), where L , b and h represents the length, width, and thickness of the beam. The beam will oscillate to reproduce the reference movement. A point to be highlighted in the project is the location, and the number of MFCs used, as these variables make up two fundamental quantities to control. Optimizing the positioning and the number of actuators is out of the scope of the present work. Figure 1 shows the geometric definitions of the MFC used.

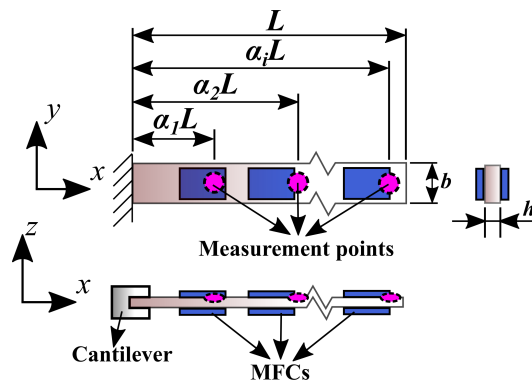


Figure 2. Structure scheme with the allocation of MFCs, dimensions and allocation of control points.

The presence of point masses positioned on the beam will not be considered. The stiffness and mass per unit length of the beam will be constant over L . This statement is not true since the rigidity and mass of the actuators are disregarded. However, due to the magnitude differences between the properties of the beam and MFCs, this hypothesis does not jeopardize the model's numerical evaluation.

The actuation is delivered by the bending moment imposed by the actuators, where effects in other directions are not considered. As it is the Euler-Bernoulli model, the equation will have the following hypotheses:

- Material homogeneity along the beam;
- Material with linear elasticity;
- Symmetry of the cross-section;
- The plane of the cross-section, at any position along the x axis, remains perpendicular after deformation;
- Rotation effects disregarded.

2.2 MODAL DOMAIN SOLUTION

The partial differential equation for vibration of an Euler-Bernoulli beam immersed in the air is given by

$$-\frac{\partial^2 M(x, t)}{\partial x^2} + c_s I \frac{\partial^5 W(x, t)}{\partial x^4 \partial t} + c_a \frac{\partial W(x, t)}{\partial t} + m \frac{\partial^2 W(x, t)}{\partial t^2} = 0, \quad (1)$$

where $W(x, t)$ is the term that represents the transverse displacement of the beam, I the moment of inertia of the structure, c_s the damping coefficient proportional to the stiffness, c_a the damping coefficient due to air, m the mass per unit length of the beam and $M(x, t)$ the internal bending moment. The hypotheses for the Euler-Bernoulli beam and the air damping were used in similar works that investigated it experimentally and shown to be consistent. Examples of these investigations can be found in Zhao and Erturk (2012), Bilgen *et al.* (2010) and Bilgen *et al.* (2008).

The term that models the moment will introduce the electromechanical coupling, responsible for translating the applied electrical voltage into actuation force. As previously mentioned, the modeling for the moment (and electromechanical coupling) was presented by Shahab (2015), where the *mixing rules* technique was used (Deraemaeker *et al.*, 2009). The modal domain solution for $W(x, t)$ is given by

$$W(x, t) = \sum_{r=1}^{\infty} \phi_r(x) \eta_r(t), \quad (2)$$

in which the term representing the vibrating modes $\phi_r(t)$, a function of the boundary conditions imposed on the beam, weighs the possibilities of dynamic behavior of the points of interest, described by the modal domain equation $\eta_r(t)$. The equations for obtaining $\phi_r(t)$ and $\eta_r(t)$ can be seen below:

$$\ddot{\eta}_r(t) + 2\zeta_r \omega_r \dot{\eta}_r(t) + \omega_r^2 \eta_r(t) = \theta_r V(t), \quad (3)$$

$$\phi_r(x) = C_r \left[-S(x) + T(x) \frac{T(L)}{Q(L)} \right], \quad (4)$$

where

$$2\zeta_r \omega_r = \frac{c_s I \omega_r^2}{E_t} + \frac{c_a}{m}, \quad \omega_r = \lambda_r^2 \sqrt{\frac{YI}{mL^4}}, \quad Q_r(x) = \cosh\left(\frac{\lambda_r}{L}x\right) + \cos\left(\frac{\lambda_r}{L}x\right),$$

$$S_r(x) = \cosh\left(\frac{\lambda_r}{L}x\right) - \cos\left(\frac{\lambda_r}{L}x\right), \quad T_r(x) = \sinh\left(\frac{\lambda_r}{L}x\right) - \sin\left(\frac{\lambda_r}{L}x\right).$$

The term C_r is the constant calculated from the orthogonality conditions, ζ_r the modal damping, ω_r the undamped natural frequency, θ_r the electromechanical modal coupling, $V(t)$ the electrical voltage at the terminals of the actuators and finally E_t the beam stiffness, given by the product of the moment of inertia of the cross-section I by the Young module of the structure Y .

The values of λ_r that distinguish the modes of vibration, natural frequencies and damping factors are given by the transcendental equation:

$$1 + \cos\lambda\cosh\lambda = 0. \quad (5)$$

Equation 3 assumes the use of a single pair of MFCs coupled to the beam. To generalize the number of MFCs used, the following relationship are defined:

$$\ddot{\eta}_r(t) + 2\zeta_r\omega_r\dot{\eta}_r(t) + \omega_r^2\eta_r(t) = \sum_{i=1}^a \theta_{ri}V_i(t), \quad (6)$$

where for a pairs of MFCs allocated, the equation of the electromechanical coupling θ_{ri} between the positions x_{ni} and x_{nf} is given by

$$\theta_{ri} = \vartheta \left. \frac{d\phi_r(x)}{dx} \right|_{x_{ni}}^{x_{nf}}. \quad (7)$$

2.3 STATE-SPACE FORMULATION

Before defining the states to be worked on, two considerations must be made:

- The mathematical description of the system is more precise as more modes of vibration are taken in the approximation of $W(x, t)$;
- The system's response approaches a continuous system's response the greater the number of points to be controlled.

The following formulation for the state space was considered, where $\mathbf{x} \in \mathbb{R}^{2ni \times 1}$ is given by:

$$\mathbf{x} = \begin{Bmatrix} \phi_1(\alpha_1 L)\eta_1 \\ \phi_1(\alpha_1 L)\dot{\eta}_1 \\ \phi_2(\alpha_1 L)\eta_2 \\ \phi_2(\alpha_1 L)\dot{\eta}_2 \\ \vdots \\ \phi_1(\alpha_2 L)\eta_1 \\ \phi_1(\alpha_2 L)\dot{\eta}_1 \\ \phi_2(\alpha_2 L)\eta_2 \\ \phi_2(\alpha_2 L)\dot{\eta}_2 \\ \vdots \end{Bmatrix} = \begin{Bmatrix} x_1 \\ x_2 \\ x_3 \\ x_4 \\ \vdots \end{Bmatrix}, \quad (8)$$

where the terms $\alpha_i, i = 1, 2, 3, \dots$ determine the points of interest, and the terms $\phi_j, j = 1, 2, 3, \dots$ the approximation of the modes of vibration. The sum of the odd index states represents the movement of the beam at the point of interest, for example, with an approximation of two modes of vibration: $W(\alpha_1 L, t) = x_1 + x_3$, $W(\alpha_2 L, t) = x_5 + x_7$ and so on.

Thus, one can define the vector of outputs $\mathbf{y} \in \mathbb{R}^{p \times 1}$ as the sum of the modal contributions, in the following form:

$$\mathbf{y} = \begin{Bmatrix} W(\alpha_1 L, t) \\ W(\alpha_2 L, t) \\ \vdots \end{Bmatrix} = \begin{Bmatrix} x_1 + x_3 + \dots + x_{2n-1} \\ x_{2n-1+2} + x_{2n-1+4} + \dots \\ \vdots \end{Bmatrix}. \quad (9)$$

The matrix equation in the state space domain will take the following form:

$$\underbrace{\dot{\mathbf{x}}}_{2ni \times 1} = \underbrace{\mathbf{A}}_{2ni \times 2ni} \underbrace{\mathbf{x}}_{2ni \times 1} + \underbrace{\mathbf{B}}_{2ni \times 3} \underbrace{\mathbf{u}}_{3 \times 1}, \quad (10)$$

$$\underbrace{\mathbf{y}}_{p \times 1} = \underbrace{\mathbf{C}}_{p \times 2ni} \underbrace{\mathbf{x}}_{2ni \times 1} + \underbrace{\mathbf{D}}_{p \times 3} \underbrace{\mathbf{u}}_{3 \times 1}, \quad (11)$$

where the input vector $\mathbf{u} \in \mathbb{R}^{3 \times 1}$ is composed of the electrical inputs yielding $\mathbf{u}^T = [V_1(t) \ V_2(t) \ V_3(t)]^T$, n is the variable that controls the number of modes of vibrating and i is the variable that controls the number of beam points.

The construction logic of the \mathbf{A} matrix is given by

$$\mathbf{A} = \begin{bmatrix} 0 & 1 & 0 & 0 & 0 & 0 & \dots \\ -\omega_1^2 & -2\zeta_1\omega_1 & 0 & 0 & 0 & 0 & \dots \\ 0 & 0 & 0 & 1 & 0 & 0 & \dots \\ 0 & 0 & -\omega_2^2 & -2\zeta_2\omega_2 & 0 & 0 & \dots \\ \dots & \dots & \dots & \dots & \dots & \dots & \ddots \end{bmatrix}. \quad (12)$$

The \mathbf{A} matrix grows horizontally and vertically as the number of modes for the approximation increases and grows diagonally as the control point number increases.

As for the construction of the \mathbf{B} matrix, the following logic is built:

$$\mathbf{B} = \begin{bmatrix} 0 & 0 & 0 \\ -\phi_1(\alpha_1 L)\tilde{\theta}_{11} & -\phi_1(\alpha_1 L)\tilde{\theta}_{21} & -\phi_1(\alpha_1 L)\tilde{\theta}_{31} \\ 0 & 0 & 0 \\ -\phi_2(\alpha_1 L)\tilde{\theta}_{12} & -\phi_2(\alpha_1 L)\tilde{\theta}_{22} & -\phi_2(\alpha_1 L)\tilde{\theta}_{32} \\ \vdots & \vdots & \vdots \end{bmatrix}. \quad (13)$$

The matrix \mathbf{B} grows vertically as the number of modes for the approximation increases. For the present work, \mathbf{B} will have 3 columns since the number of MFCs that will act on the beam will be 3 pairs.

Finally, for the matrix \mathbf{C} , the following logic is built:

$$\mathbf{C} = \begin{bmatrix} 1 & 0 & 1 & 0 & 1 & 0 & \dots \\ \vdots & \vdots & \vdots & \vdots & \vdots & \vdots & \dots \end{bmatrix}. \quad (14)$$

The matrix \mathbf{C} grows horizontally as the number of modes for the approach increases and grows vertically as the number of beam control points increases.

3. OPTIMAL CONTROL STRATEGY

The adopted control strategy (MPC) revolves around the optimization of an objective function (also known as a cost function) (Wang, 2009; Camacho and Alba, 2013). Some works had used the MPC in control of beams with piezoelectric performance, as in Rosenzweig *et al.* (2018). Other control possibilities involving piezoelectric actuators were also investigated, such as control based on Prony algorithm (Sheng *et al.*, 2016), LQR (Jarzyna *et al.*, 2012) and through fuzzy logic (Zhang *et al.*, 2016). In the present paper, the cost function based on the quadratic error is used.

3.1 COST FUNCTION

Let be a system of differential equations in the time interval T (Bryson, 1975; Snyman *et al.*, 1992; Franklin *et al.*, 2002):

$$\dot{\mathbf{x}}(t) = f(t, \mathbf{x}(t), \mathbf{u}(t)), \quad (15)$$

where $\mathbf{x}(t) \in \mathbb{R}^{2ni \times 1}$ and $\mathbf{u}(t) \in \mathbb{R}^{3 \times 1}$ represent the state and control, respectively, with t being the time variable. For optimal control problems with constraints, considering discrete systems, with the quadratic error as an objective function (Hedengren *et al.*, 2014), the following function is determined:

$$\min_{\mathbf{x}, \mathbf{y}, \mathbf{u}} J = \min_{\mathbf{x}, \mathbf{y}, \mathbf{u}} \sum_{k=1}^{N_p-1} (\mathbf{y}(k) - \mathbf{y}_t(k))^T \mathbf{w}_t (\mathbf{y}(k) - \mathbf{y}_t(k)) + \mathbf{y}(k)^T \mathbf{w}_y + \mathbf{u}(k)^T \mathbf{w}_u + \Delta \mathbf{u}^T \mathbf{w}_{\Delta \mathbf{u}} \Delta \mathbf{u}, \quad (16)$$

subject to

$$0 = h\left(\frac{\Delta \mathbf{x}}{\Delta t}, \mathbf{x}, \mathbf{y}, \mathbf{u}\right), \quad 0 \leq g\left(\frac{\Delta \mathbf{x}}{\Delta t}, \mathbf{x}, \mathbf{y}, \mathbf{u}\right), \quad \tau_c \frac{\Delta \mathbf{y}_t}{\Delta t} + \mathbf{y}_t = \mathbf{sp},$$

where J represents the objective function to be minimized, \mathbf{y} is the model's predictions, \mathbf{y}_t is the reference trajectory, \mathbf{w}_t represents the penalty given to the reference trajectory, $\mathbf{w}_{\Delta\mathbf{u}}$ represents the movement penalty of the manipulated variable, w_u and w_y represent the input and output weights, \mathbf{y} , \mathbf{x} and \mathbf{u} are the outputs, states and inputs, respectively, $\Delta\mathbf{u}$ the change in the manipulated variable, N_p the number of samples in the prediction horizon, and h and g the restrictions of equality and inequality, for every $t \in [0, T]$. The term $\mathbf{sp}(t_i)$ represents the setpoint at time t_i , such that the applied control considers it as a fixed reference and the speed with which $\mathbf{y}_t(t_i)$ reaches $\mathbf{sp}(t_i)$ is controlled by τ_c , which, in this study, is set as a low value, for a convergence to $\mathbf{sp}(t_i)$ quickly, ensuring that the system follows the moving reference.

In the present study, only restrictions in \mathbf{u} (inputs) were used, with lower and upper limits of electrical voltage equal to -500 and 1500 Volts, respectively, constituting the inequality constraint g . A restriction was also used for the increment (in Volts) for the input, given by $\Delta\mathbf{u}_{max} = 50$ V. In addition to these restrictions, the equations that govern the model studied in state-space constitute the restrictions shown in h .

4. NUMERICAL RESULTS

For all simulated cases, a 3-second simulation time with 1500 samples was used, and in 70% of the total time, the setpoint was reset to check the efficiency of the controller for both a moving and fixed reference. The moving reference was given by the third mode of vibration of the structure normalized for a maximum amplitude of 2 cm (in L). Three pairs of MFCs were used, located in the positions 0.04L, 0.6L, and L .

Three situations were considered for simulation, the first with 1 control point, the second with 3 control points, and finally with 5 control points. Table 1 summarizes information about the number of vibration modes used in each case, together with the allocation of control points.

Table 1. Conditions for simulation considering the number of points and number of modes considered.

Condition	Number of control points	Allocation of points	Number of modes
1	1	[L]	3
2	3	[0.2L, 0.5L, L]	5
3	5	[0.2L, 0.4L, 0.6L, 0.8L, L]	5

The physical and geometrical parameters of the beam are given in the Tab. 2. An MFC (actuator) of the type M-2814-P1 was used, and specifications can be found in the manufacturer's datasheet (Smart Material, 2003 -2021). In addition, information about the parameters used in the control project is displayed in Tab. 3. The GEKKO (Beal *et al.* (2018)) optimization library was used to apply the control strategy.

Table 2. Physical parameters adopted in the simulations.

Parameter	Description	Value	Unit
L	Beam length	0.40	m
b	Beam width	0.02	m
h	Beam thickness	3×10^{-4}	m
ρ	Beam material density	1340	kg/m ³
E	Modulus of elasticity of the beam material	3×10^9	Pa
ζ_1	Damping rate for the first mode	0.01	Dimensionless
ζ_2	Damping rate for the second mode	1.2×10^{-2}	Dimensionless
coupling	Electromechanical coupling disregarding the beam thickness	2×10^{-6}	Nm/V

Table 3. Parameters adopted in the design of the control.

Parameter	Description	Value	Unit
τ_c	Time constant for controlled variable response	1×10^{-5}	s
N_p	Prediction horizon	80	Dimensionless
w_t	Penalty outside reference trajectory	1	Dimensionless
w_y	Weight on output	1	Dimensionless
w_u	Weight on input	0	Dimensionless
$w_{\Delta\mathbf{u}}$	Manipulated variable movement penalty	0	Dimensionless

The first simulation is the least complex case, with only one point of interest and three modes for the approach, yielding 6 states to be controlled. The desired output (movement reference in L) is a sinusoid with an amplitude of 2 cm (Fig. 3).

The dynamic behavior of the point follows the desired reference with a small quadratic error, indicating an efficiency in choosing the cost function and the control parameters. Except for the start of the simulation and the change from moving to a fixed reference (close to 2 seconds), the quadratic error remains null, which indicates the quality of control.

It appears that the inputs also show harmonic behavior, with the MFC number 2 reaching the lower limit of electrical voltage. The actuator in position 1, closest to the cantilever, is the one that least consumes energy in the process in relation to the others.

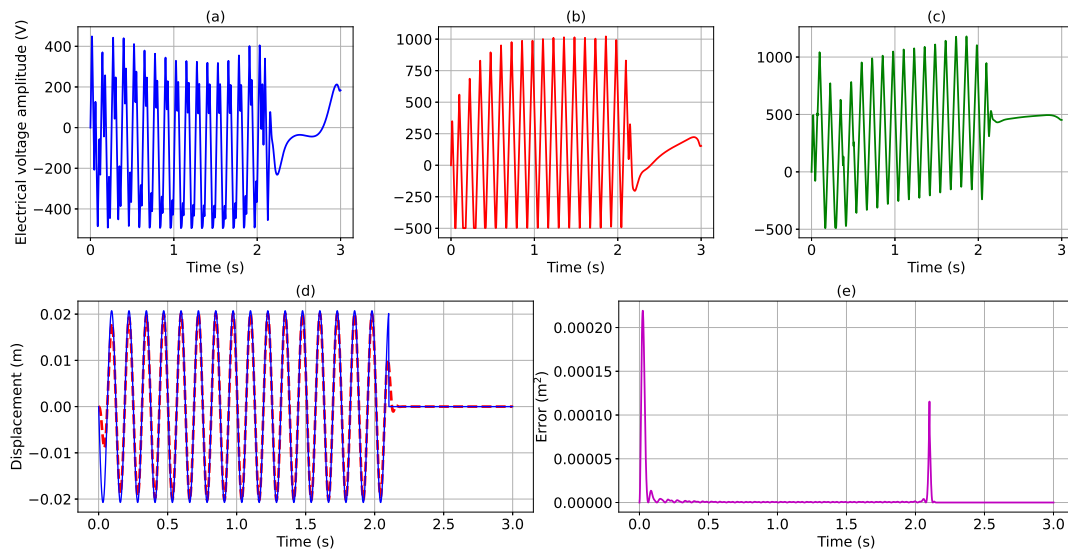


Figure 3. Condition 1. In (a), (b) and (c) the electrical voltages obtained by the control strategy in the positions of MFCs 1, 2 and 3 respectively, in (d) in blue (—) the desired output and in red (---) the output obtained by the model and in (e) the calculated quadratic error.

The second simulation raises the computational cost compared to the first: 3 control points and 5 modes, totaling 30 states. Input references were also sinusoidal, with different amplitudes at points of interest (Fig. 4). As can be seen, the error obtained has an order of magnitude smaller than the reference or the output of the system. However, due to the increase in the number of states, the error also increases: the dynamic behavior of the point L does not follow the reference imposed in the same way as the simulation under the condition 1.

The inputs do not follow a harmonic pattern as in Fig. 3, since with more points (and states) to be controlled, the demand on the actuators is greater. It is also noted that for control points 1 and 3, the output was smaller in amplitude than the reference during the entire simulation period, while for control point 2 (located at $0.5L$ from the cantilever), the output was greater than the reference. This indicates that the control action was more conservative in points 1 and 3 and allowed greater displacements in 2, given the configuration of the MFCs along the beam.

The third simulation is the case with the highest computational cost: 5 control points and 5 modes, totaling 50 states. The increase in the error observed between the first and the second simulation also occurs between the second and third, to the detriment of the increase in the number of states. The increase in the number of control points should be weighted by the project's need, as, as noted, the output error increases as i increases (Fig.5). Another consideration that must be made, concerns the possibilities of physical references: the ways of vibrating $\phi(x)$ limit the possible behaviors of the beam.

Although it did not reach the setpoints in amplitude, the control was able to reproduce the behavior of the frequency reference. Among the possible solutions to make the system reach the desired reference at all points would be to study the allocation of MFCs and find the optimal position that maximizes performance. In addition, more modes of vibration could be included to represent the structure, with increased computational cost. Another possible strategy would be to increase the number of MFCs or increase the applied voltage restriction limits (if this is physically possible) depending on the type of MFC used.

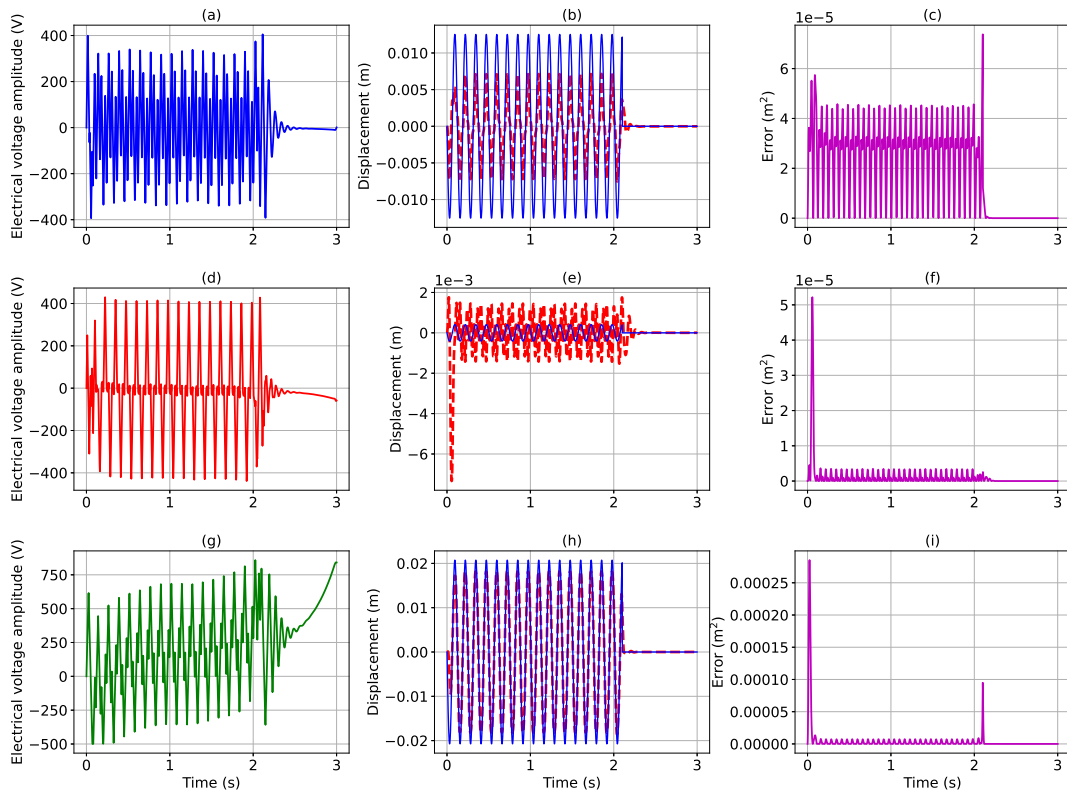


Figure 4. Condition 2. In (a), (d) and (g) the electrical voltages obtained by the control strategy in the positions of MFCs 1, 2 and 3 respectively, in (b), (e) and (h) in blue (—) the desired output and in red (---) the output obtained by the model for the first, second and third points, respectively $[0.2L, 0.5L$ and $L]$ and in (c), (f) and (i) the quadratic error calculated following the same order as the points.

5. CONCLUSIONS

The application of the presented method, although it has an initial motivation in the control of vibrations, can be used in tracking dynamic behaviors in elastic systems, where examples can be found in some robotic systems that present low structural stiffness (also known as soft robots).

The beam control is able to reproduce the desired behavior, preserving the approximation for the rigidity of the structure (which disregards the effects of the allocation of the MFCs). The control strategy is efficient, but the computational cost of the optimization can become significantly high depending on the number of modes and the number of points that are used in the model approximation. The simulation is consistent with the expected results; however, due to the character of the approximations made, the model lacks experimental validation, especially the relation of points and modes taken to approach the model.

Among some points to be further investigated, it is essential to highlight the importance of the MFCs' allocation along the beam. These localizations influence the control output amplitude, variations in the reference, other ways of vibrating the structure, or some other reference. In addition, investigations about structural and control modifications such as beam length, width, thickness, control strategies, etc., should also be carried out.

Specifically, regarding control, the objective function used, given by the quadratic error, could be replaced by an 11-norm objective function with lower and upper limits that can bring different and comparable results, constituting another parameter to be taken into account in the analysis. One could also build some kind of metric to evaluate the quality of the output values compared to the reference values, such as a mean square error, for example, and the time required for the control to reach the desired trajectory.

The generalization of the problem presented, whether to the damping rate provided by other means (fluids other than air) or to different boundary conditions to the end (free or cantilever ends), also constitutes suggestions for future work. Although the generalization proposals increase the complexity of the equations, the elaboration of the state space will follow the same model.

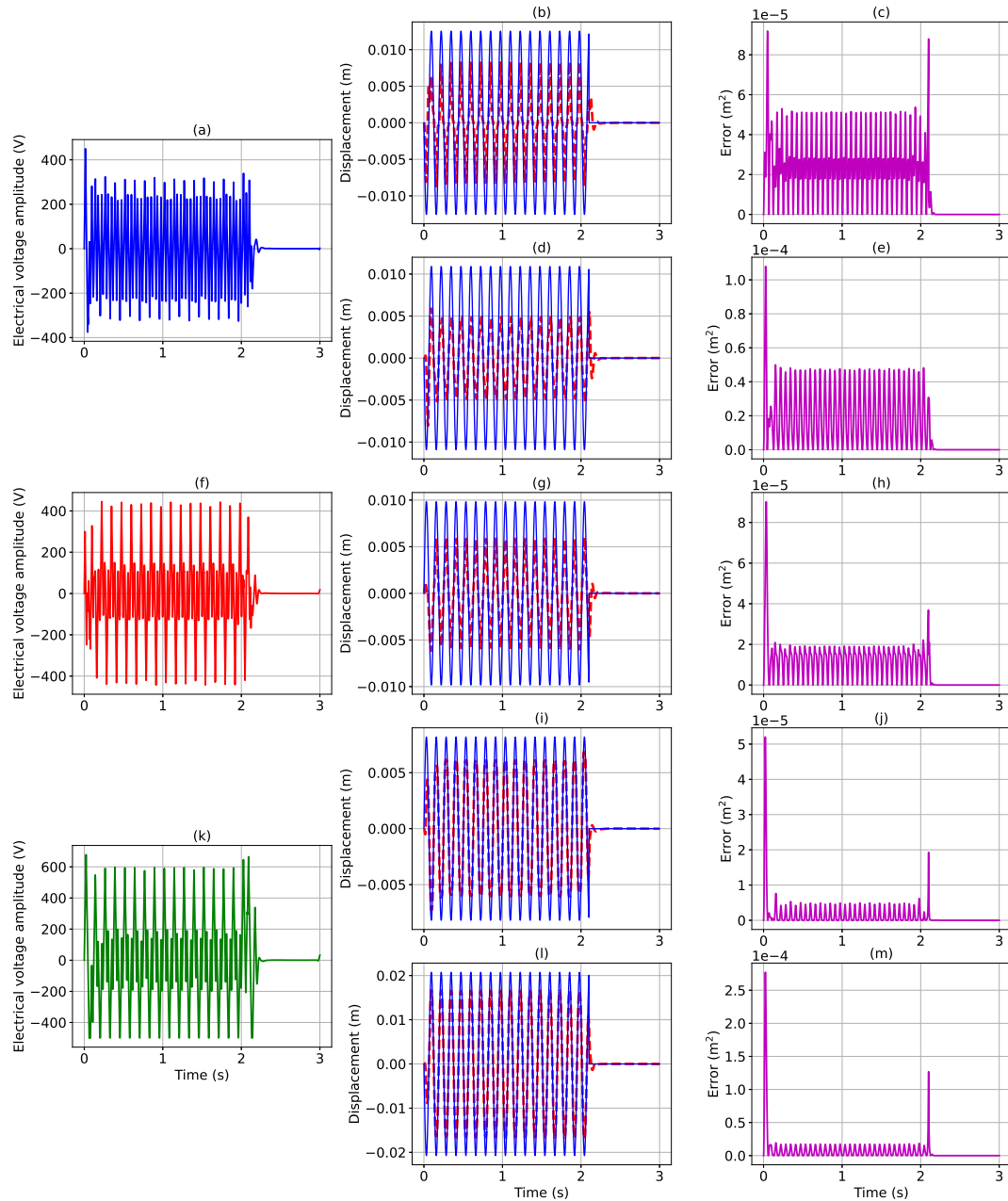


Figure 5. Condition 3. In (a), (f) and (k) the electrical voltages obtained by the control strategy in the positions of MFCs 1, 2 and 3 respectively, in (b), (d), (g), (i) and (l) in blue (—) the desired output and in red (---) the output obtained by the model for the first, second, third, fourth and fifth points, respectively [0.2L, 0.4L, 0.6L, 0.8L and L] and in (c), (e), (h), (j) and (m) the quadratic error calculated following the same order of points.

6. REFERENCES

- Balachandran, B. and Magrab, E.B., 2018. *Vibrations*. Cambridge University Press.
- Beal, L.D., Hill, D.C., Martin, R.A. and Hedengren, J.D., 2018. “Gekko optimization suite”. *Processes*, Vol. 6, No. 8, p. 106.
- Bent, A.A., 1997. *Active fiber composites for structural actuation*. Ph.D. thesis, Massachusetts Institute of Technology.
- Bilgen, O., Erturk, A. and Inman, D.J., 2010. “Analytical and experimental characterization of macro-fiber composite

- actuated thin clamped-free unimorph benders”. *Journal of Vibration and Acoustics*, Vol. 132, No. 5.
- Bilgen, O., Erturk, A., Inman, D.J. and Kochersberger, K.B., 2008. “Macro-fiber composite actuated thin clamped-free benders and thin simply-supported morphing airfoils”. In *19th International Conference on Adaptive Structures and Technologies*. Vol. 6.
- Bryson, A.E., 1975. *Applied optimal control: optimization, estimation and control*. CRC Press.
- Camacho, E.F. and Alba, C.B., 2013. *Model predictive control*. Springer Science & Business Media.
- Deraemaeker, A., Nasser, H., Benjeddou, A. and Preumont, A., 2009. “Mixing rules for the piezoelectric properties of macro fiber composites”. *Journal of intelligent material systems and structures*, Vol. 20, No. 12, pp. 1475–1482.
- Erturk, A. and Inman, D.J., 2011. *Piezoelectric energy harvesting*. John Wiley & Sons.
- Franklin, G.F., Powell, J.D., Emami-Naeini, A. and Powell, J.D., 2002. *Feedback control of dynamic systems*, Vol. 4. Prentice hall Upper Saddle River, NJ.
- Gillespie, M.T., Best, C.M. and Killpack, M.D., 2016. “Simultaneous position and stiffness control for an inflatable soft robot”. In *2016 IEEE international conference on robotics and automation (ICRA)*. IEEE, pp. 1095–1101.
- Hedengren, J.D., Shishavan, R.A., Powell, K.M. and Edgar, T.F., 2014. “Nonlinear modeling, estimation and predictive control in apmonitor”. *Computers & Chemical Engineering*, Vol. 70, pp. 133–148.
- Huang, D.d., 2017. “Finite element modelling of macro fiber composite with interdigitated electrode for engineering applications”. In *2017 Symposium on Piezoelectricity, Acoustic Waves, and Device Applications (SPAWDA)*. IEEE, pp. 463–470.
- Jarzyna, W., Augustyniak, M., Warmiński, J. and Bocheński, M., 2012. “State control with lqr algorithms applied in vibration damping of cantilever beam”. In *2012 15th International Power Electronics and Motion Control Conference (EPE/PEMC)*. IEEE, pp. DS1c–8.
- Leo, D.J., 2007. *Engineering analysis of smart material systems*. John Wiley & Sons.
- Rimašauskienė, R., Jūrėnas, V., Radzienski, M., Rimašauskas, M. and Ostachowicz, W., 2019. “Experimental analysis of active–passive vibration control on thin-walled composite beam”. *Composite Structures*, Vol. 223, p. 110975.
- Rosenzweig, P., Kater, A. and Meurer, T., 2018. “Model predictive control of piezo-actuated structures using reduced order models”. *Control Engineering Practice*, Vol. 80, pp. 83–93.
- Shahab, S. and Erturk, A., 2016. “Electrohydroelastic euler–bernoulli–morison model for underwater resonant actuation of macro-fiber composite piezoelectric cantilevers”. *Smart Materials and Structures*, Vol. 25, No. 10, p. 105007.
- Shahab, S., 2015. *Vibration energy harvesting, biomimetic actuation, and contactless acoustic energy transfer in a quiescent fluid domain*. Ph.D. thesis, Georgia Institute of Technology.
- Sheng, X., Kong, Y., Zhang, F. and Yang, R., 2016. “Identification for active vibration control of flexible structure based on prony algorithm”. *Shock and Vibration*, Vol. 2016.
- Smart Material, 2003 -2021. “MFC P1, F1 and S1 types (d33 effect), elongator”. URL <https://www.smart-material.com/MFC-product-P1V2.html>.
- Snyman, J., Frangos, C. and Yavin, Y., 1992. “Penalty function solutions to optimal control problems with general constraints via a dynamic optimisation method”. *Computers & Mathematics with Applications*, Vol. 23, No. 11, pp. 47–55.
- Wang, L., 2009. *Model predictive control system design and implementation using MATLAB®*. Springer Science & Business Media.
- Wilkie, W.K., Bryant, R.G., High, J.W., Fox, R.L., Hellbaum, R.F., Jalink Jr, A., Little, B.D. and Mirick, P.H., 2000. “Low-cost piezocomposite actuator for structural control applications”. In *Smart structures and materials 2000: industrial and commercial applications of smart structures technologies*. International Society for Optics and Photonics, Vol. 3991, pp. 323–334.
- Zhang, Y., Luo, Y. and Zhang, X., 2016. “Nonlinear vibration control of a piezoelectric beam with a fuzzy logic controller”. *International Journal of Applied Electromagnetics and Mechanics*, Vol. 52, No. 1-2, pp. 251–260.
- Zhao, S. and Erturk, A., 2012. “Electroelastic modeling and experimental validations of piezoelectric energy harvesting from broadband random vibrations of cantilevered bimorphs”. *Smart Materials and Structures*, Vol. 22, No. 1, p. 015002.

Acknowledgement

This research is supported by FAPESP 2018/21336-0 and FAPESP 2018/15894-0. Moreover, Arthur B. Silva, Lucas Z. Tahara and Maíra M. da Silva are grateful for their research grants, CAPES 88887.498358/2020-00, CNPq 140800/2020-4 and CNPq 301338/2018-3, respectively.

7. RESPONSIBILITY NOTICE

The author are solely responsible for the printed material included in this paper.